

Anodised TiO₂ nano-tubes: voltage ramp influence on the nano-structured oxide and investigation of phase changes promoted by thermal treatments

D. Regonini¹, C. R. Bowen¹, R. Stevens¹, D. Allsopp², and A. Jaroenworarluck³

¹ Materials Research Centre, Dept. of Mechanical Engineering, University of Bath, Claverton Down Road, Bath BA2 7AY, UK

² Dept. of Electronic & Electrical Engineering, University of Bath, Claverton Down Road, Bath BA2 7AY, UK

³ MTEC: National Metal and Materials Technology Center, 114 Thailand Science Park, Paholyothin Rd., Klong 1, Klong Luang, Pathumthani 12120, Thailand

Received 11 October 2006, accepted 22 March 2007

Published online 23 May 2007

PACS 61.46.Fg, 68.37.Hk, 68.37.Lp, 81.40.Tv

TiO₂ nano-tubes have been generated by anodising commercially pure (99.6%) titanium in a 1 M solution of Na₂SO₄ which contains a small amount of NaF (0.1–1 wt%). The use of an initial voltage ramp, prior to the application of a constant voltage to the cell, led to an increase in the thickness of the nano-tube layer. The thermal stability of the nano-tube layer has also been evaluated by annealing at a variety of temperatures, from 200 to 600 °C. Scanning Electron Microscopy (SEM) of the annealed nano-tubes indicate that they are stable up to 500 °C. Raman spectroscopy was performed to monitor and evaluate the changes in the crystal structure promoted by the thermal treatments. The as-prepared nano-tubes are amorphous, while anatase begins to form at 300 °C and rutile is found at 550 °C, a temperature at which the nano-tubes begin to collapse. Initial results obtained by characterising the as-prepared nano-tubes with Transmission Electron Microscopy (TEM) are also discussed.

Anodised TiO₂ nano-tubes: voltage ramp influence on the nano-structured oxide and investigation of phase changes promoted by thermal treatments

D. Regonini^{*1}, C. R. Bowen¹, R. Stevens¹, D. Allsopp², and A. Jaroenworarluck³

¹ Materials Research Centre, Dept. of Mechanical Engineering, University of Bath, Claverton Down Road, Bath BA2 7AY, UK

² Dept. of Electronic & Electrical Engineering, University of Bath, Claverton Down Road, Bath BA2 7AY, UK

³ MTEC: National Metal and Materials Technology Center, 114 Thailand Science Park, Paholyothin Rd., Klong 1, Klong Luang, Pathumthani 12120, Thailand

Received 11 October 2006, accepted 22 March 2007

Published online 23 May 2007

PACS 61.46.Fg, 68.37.Hk, 68.37.Lp, 81.40.Tv

TiO₂ nano-tubes have been generated by anodising commercially pure (99.6%) titanium in a 1 M solution of Na₂SO₄ which contains a small amount of NaF (0.1–1 wt%). The use of an initial voltage ramp, prior to the application of a constant voltage to the cell, led to an increase in the thickness of the nano-tube layer. The thermal stability of the nano-tube layer has also been evaluated by annealing at a variety of temperatures, from 200 to 600 °C. Scanning Electron Microscopy (SEM) of the annealed nano-tubes indicate that they are stable up to 500 °C. Raman spectroscopy was performed to monitor and evaluate the changes in the crystal structure promoted by the thermal treatments. The as-prepared nano-tubes are amorphous, while anatase begins to form at 300 °C and rutile is found at 550 °C, a temperature at which the nano-tubes begin to collapse. Initial results obtained by characterising the as-prepared nano-tubes with Transmission Electron Microscopy (TEM) are also discussed.

© 2007 WILEY-VCH Verlag GmbH & Co. KGaA, Weinheim

1 Introduction

The generation of porous oxide films by metallic anodisation have recently become of significant interest, particularly after Masuda and Fukuda produced a self-ordered nano-porous array of alumina by a two step anodisation process [1]. The formation mechanism of porous alumina is now well established and understood, however the generation of nano-porous oxides by anodising other metals, such as Ti, is still in its infancy. In 1999, Zwilling et al. [2] reported the formation of nano-porous titania in a dilute HF solution. The formation of anodised titania nano-tubes was first discussed in 2001 by Grimes et al. [3], using dilute HF as the electrolyte. Titanium oxide has attracted particular interest because of its properties that make it useful in many fields such as biomedical [4–6], gas-sensing [7–10], photo-catalysis [11–18], solar cells [19–25] and photonic crystal devices [26]. Taking porous alumina as an example, scientists have proposed a growth mechanism based on field-enhanced dissolution [27, 28], while more recently a mechanism based upon chemical dissolution phenomena has been suggested [29, 30]. The general understanding of the process has helped to improve the experimental set-up, achieve higher homogeneity and generate thicker nano-tube layers up to 7 μm [31]. However, research on titania nano-

* Corresponding author: e-mail: D.Regonini@bath.ac.uk, Phone: +44 (0)1225 383062, Fax: +44 (0)1225 386928

tubes is relatively new and many other aspects need to be investigated before developing a clear, general overview of the process. In this paper, results and observations, which provide new insight into the anodised titania nano-tube growth mechanism, are presented.

2 Experimental

Commercially pure (99.6%, 0.5 mm thick) Ti sheets were mechanically polished to generate a mirror-like surface (free of scratches) then placed in a Teflon sample holder, leaving 1 cm² of Ti surface exposed to the electrolyte as the anode. A Pt mesh was used as a counter electrode. Prior to anodisation, the samples were ultrasonically cleaned in an isopropyl alcohol bath. A 1 M solution of Na₂SO₄ with a small amount of added NaF (from 0.1 to 1 wt%) was used as an electrolyte. Experiments were carried out at either a constant voltage of 20 V or with a voltage ramp (from 100 to 1000 mV/sec) from the open circuit potential to 20 V before holding the potential at constant value. The potential was applied using a Keithley 236 power supply, interfaced with a PC to monitor the current–time transient during anodisation. Anodised samples were subsequently annealed in air at temperatures ranging from 200 to 600 °C for 3 h (heating rate 4 °C/min) to investigate stability of the nano-tubes and changes in the crystal phases. Samples were characterised by Scanning Electron Microscopy (SEM, model JEOL JSM6480LV), Transmission Electron Microscopy (TEM, model, JEOL JEM2010) and Raman Spectroscopy (Renishaw RM2000).

3 Results and discussions

Nano-tubes were obtained using NaF concentrations below 0.3 wt%, but the best results in terms of self-organisation of the tubes were observed when using a fluorine concentration between 0.5 and 1 wt%. Consequently, 0.5 wt% of NaF, supported by a 1 M solution of Na₂SO₄, was chosen as a standard electrolyte for our experiments and this represented the best compromise between the need to dissolve the oxide to generate tubes and the need to preserve the oxide, which otherwise would have become too thin. When using a constant voltage (20 V) and no voltage ramp, the maximum nano-tube layer thickness was ~0.8 μm, as shown in the SEM image, Fig. 1a. The layer thickness remained unchanged even when the anodising time was increased up to 5 h. The current-transient registered during the experiment is shown in Fig. 1b. At first, the current quickly decreases to a minimum value due to the formation of a dense barrier layer oxide based complex, which grows up to 50 nm [32]. The current subsequently rises to a maximum during the pore nucleation phase, and finally becomes constant indicating equilibrium between oxide dissolution and growth. It is worth noting that these changes occur within the first few seconds of the anodisation process and dissolution–growth equilibrium is rapidly achieved. For this reason, the thickness of the tubular layer is limited to 0.8 μm. The control of the chemical dissolution parameters

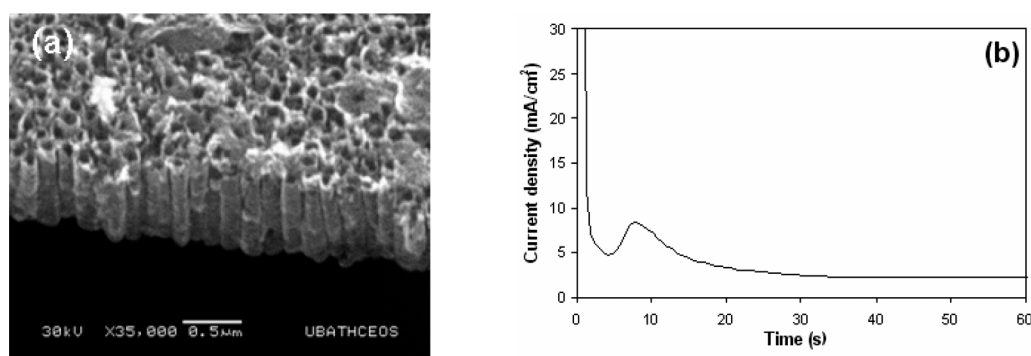


Fig. 1 SEM cross sectional view image (a) of anodised nano-tubes prepared under potentiostatic condition at 20 V, and (b) correspondent current-transient registered.

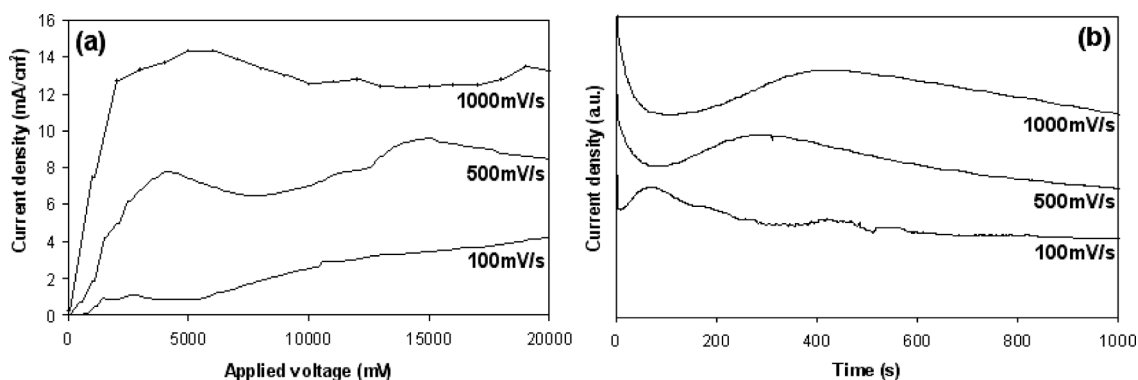


Fig. 2 (a) Polarisation curves registered at different sweep rates, 100, 500 and 1000 mV/s and (b) current transient registered at 20 V, after the initial voltage ramp was finished.

becomes crucial in order to generate a pH gradient between the mouth and the base of the tubes and produce a thicker layer [30, 31].

An alternative situation can be created by using a voltage ramp from the open circuit potential to 20 V, before finally applying a constant voltage of 20 V. Figure 2a and b show the polarisation curves for sweep rates between 100 and 1000 mV/sec and the current transient registered at 20 V once the ramp has terminated, respectively. Figure 2a shows that for all sweep rates, the current becomes approximately constant (after an initial increase) indicating the formation of a barrier type titania layer. The increased resistance provided by this thickening layer is counterbalanced by the increasing voltage and by pore nucleation, which is promoted by fluoride ions. Once the voltage ramp is complete, Fig. 2b, the current then falls in all the curves to a minimum, where the barrier layer reaches its maximum thickness. At this point, the increasing resistance developed by the oxide cannot be balanced by an increase in voltage, which has reached its maximum value of 20 V. However, nucleation of pores continues and the current increases to a maximum before becoming constant, when the equilibrium between oxide generation and dissolution is achieved. Figure 2b clearly shows how by increasing the sweep rate, the time to reach the equilibrium between oxide formation and dissolution is retarded and, as a result, a thicker nano-tube layer can be synthesised.

A top view (with higher magnification in the inset) and a cross sectional view of SEM images of nano-tubes prepared using an initial sweep rate of 100 mV/s from the open circuit potential to 20 V are shown in Fig. 3a and b, respectively. The nano-tube thickness is $\sim 1.5 \mu\text{m}$. The chemical dissolution rate of the titanium oxide is influenced by the electrolytic pH [33]. It has been previously reported that the use of a voltage ramp establishes a pH gradient between the bottom (low pH) and the mouth (high pH) of the pores, creating the conditions for the growth of thicker tubes [30]. Considering Figs. 2 and 3, it emerges that when using a voltage ramp, nucleation of the pores takes place while the barrier layer is relatively thin. This may play a role in the generation of a pH gradient between the bottom and the mouth of the nano-structure. In fact, in the absence of voltage ramp, nucleation takes place on the thicker 50 nm barrier layer, leading to the formation of a thinner layer of nano-tubes. Similar results, in terms of morphology and thickness, were obtained when using a sweep rate of 500 and 1000 mV/s. However, for these two higher sweep rates, sections of the oxide layer were found in the electrolyte after the anodisation. Although further investigations are required to clarify why regions of the oxide layer detach from the substrate, this indicates that the oxide layer produced with sweep rates of 500 and 1000 mV/s may have been thicker than the one produced at 100 mV/s. This is also suggested by the current transients of Fig. 2b, where at higher sweep rates (500 and 1000 mV/s), the time to reach equilibrium is more retarded than at 100 mV/s. Finally, as can be seen in Fig. 3a, the initial sweep rate does not affect the diameter of the tubes ($\sim 100 \text{ nm}$), which is mainly dependent by the applied voltage [34].

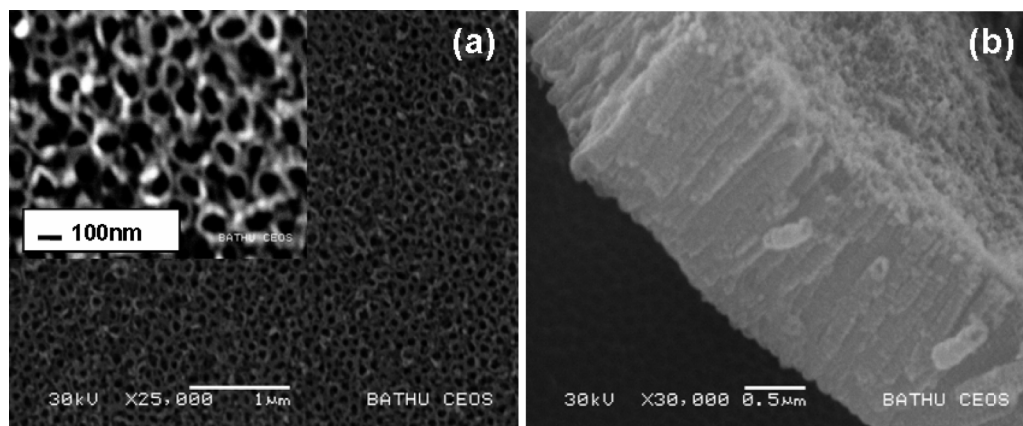


Fig. 3 Front view (a) and cross sectional view (b) SEM images of anodised titania nano-tubes prepared in 1 M Na_2SO_4 , 0.5 wt% NaF, by applying an initial voltage ramp (from the open circuit potential to 20 V) of 100, before holding the voltage constant at 20 V for 5 h.

Preliminary TEM investigation, performed on a sample anodised in 1 M Na_2SO_4 + 0.5 wt% of NaF for 30 minutes at 20 V, are shown in Fig. 4. It can be seen how pores are interconnected in the early stage of the anodisation process, before the formation of the final nano-tube layer. The connection of the cavities optimises the passage of the current through the insulating oxide layer. A critical current value has been proposed to determine whether a pore will survive or not during the anodisation process [32]. It can be hypothesised that by using an initial sweep rate, since deeper pores can be generated, the number of surviving pores is higher; therefore, once they link up together, they can also generate longer tubes.

The thermal stability of anodised titania nano-tubes and related phase changes have also been investigated by Raman spectroscopy (Fig. 5a) and SEM analysis (Fig. 5b). As prepared nano-tubes are amorphous and, once heated, they remain stable up to 500 °C, as previously reported [35, 36].

As can be seen in Fig. 5a, from Raman spectra registered for samples annealed at different temperatures, the crystal structure is anatase from 300 up to 500 °C, while the rutile phase appears at 550 °C. From the SEM images, it seems that most of the nano-tubes collapse at 550 °C and completely disappear at 600 °C. It is not clear if the nano-tube collapse is related with the changes in the crystal structure. Further TEM investigations are underway to clarify this aspect. The possibility of generating anatase

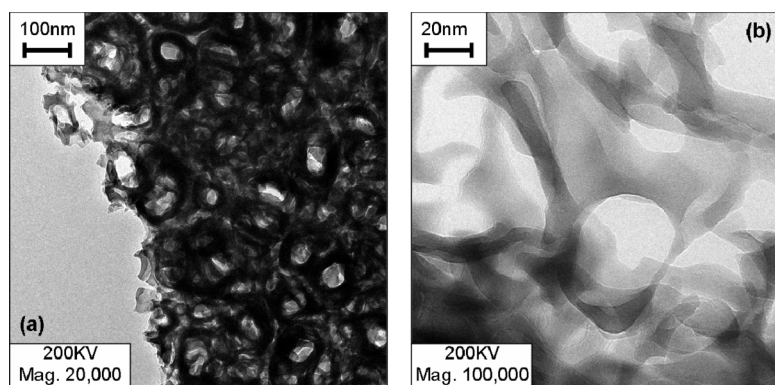


Fig. 4 TEM images of a sample prepared at 20 V in 1 M Na_2SO_4 , 0.5 wt% NaF. Anodisation was stopped after 30', in order to evaluate the morphology of the structure before the nano-tubes layer was completely formed.

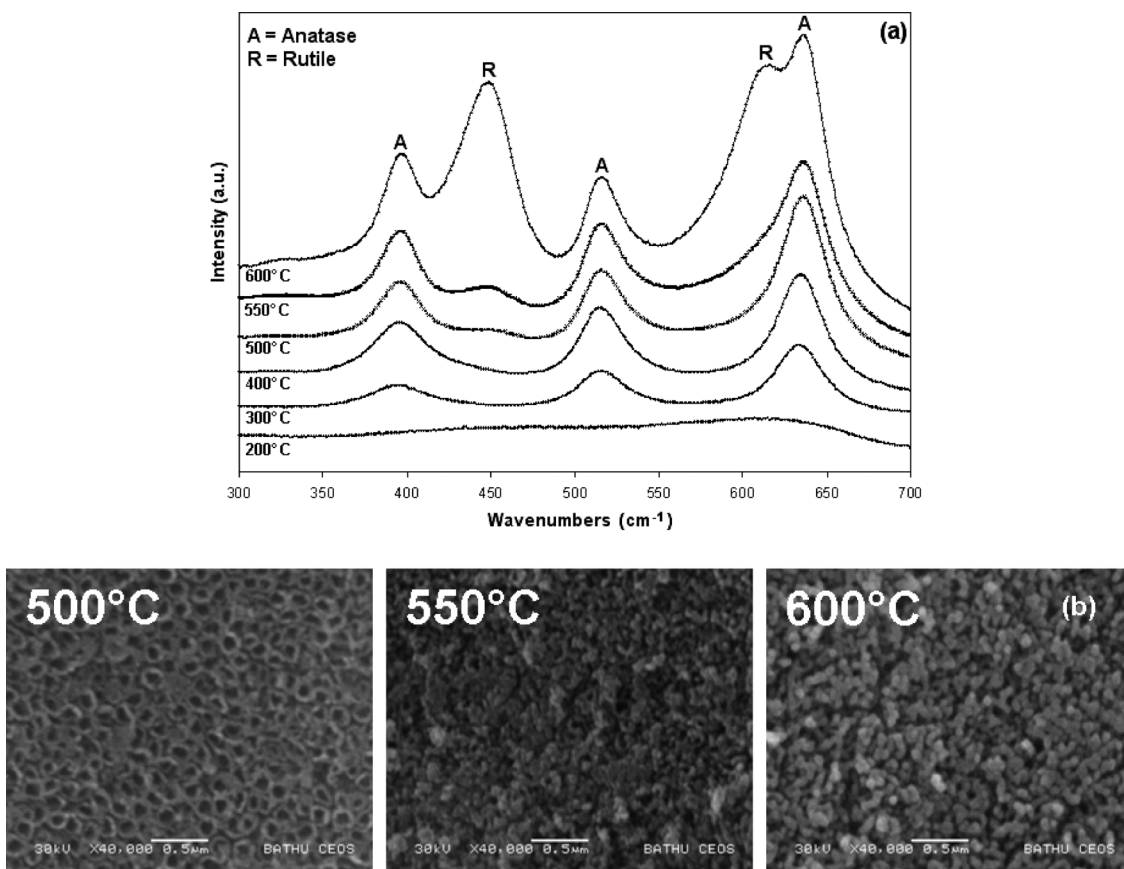


Fig. 5 Raman spectroscopy (a) showing crystal phase changes in anodised titania nano-tubes annealed in air at different temperature, from 200 to 600 °C and (b) SEM images of samples annealed at 500, 550 and 600 °C.

crystals, without destroying the nano-tubular morphology, may be particularly interesting for dye sensitized solar cell (DSSCs) applications [37].

4 Conclusions

In conclusion, the generation of anodised titania nano-tubes in a fluorine based electrolyte has been investigated. Since it is not possible to produce different chemical dissolution rates at the mouth and bottom of the nano-tubes, the thickness of the layer is limited to 0.8 μm when working under potentiostatic conditions. The use of an initial voltage ramp allows pore nucleation and growth to occur when the barrier layer oxide is relatively thin. This helps to generate cavities and leads to thicker tube layers since the time for reaching equilibrium between oxide dissolution and growth is retarded. TEM analysis shows how cavities and pores are interconnected before the generation of well-defined tubes. Nano-tubes are observed to be stable up to 500 °C and undergo transition from an amorphous phase to anatase without change of morphology. Among the possible applications, the use of anodised titania nano-tubes in dye sensitised solar cells will be investigated in the future.

Acknowledgements The Royal Academy of Engineering, The Worshipful Company of Armourers and Brasiers and Novelis are gratefully acknowledged for the financial contribution provided in support of this work. The Interface Analysis Centre of the Bristol University, where Raman measurements were performed, is also acknowledged.

References

- [1] H. Masuda and K. Fukuda, *Science* **268**, 1466 (1995).
- [2] V. Zwilling, E. Darque-Ceretti, A. Boutry-Forveille, D. David, M. Y. Perrin, and M. Aucouturier, *Surf. Interface Anal.* **27**, 629 (1999).
- [3] D. Gong, C. A. Grimes, O. K. Varghese, W. Hu, R. S. Singh, Z. Chen, and E. C. Dickey, *J. Mater. Res.* **16**, 3331 (2001).
- [4] X. Zhu, K. H. Kim, and Y. Jeong, *Biomater.* **22**, 2199 (2001).
- [5] B. Yang, M. Uchida, H. M. Kim, X. Zhang, and T. Kokubo, *Biomater.* **25**, 1003 (2004).
- [6] S. H. Oh, R. R. Finões, C. Daraio, L. H. Cen, and S. Jin, *Biomater.* **26**, 4938 (2005).
- [7] G. K. Mor, M. A. Carvalho, M. V. Pishko, and C. A. Grimes, *J. Mater. Res.* **19**, 628 (2004).
- [8] O. K. Varghese and C. A. Grimes, *J. Nanosci. Nanotechnol.* **3**, 277 (2003).
- [9] O. K. Varghese, D. Gong, M. Paulose, K. G. Ong, and C. A. Grimes, *Sens. Actuators B* **93**, 338 (2003).
- [10] O. K. Varghese, D. Gong, M. Paulose, K. G. Ong, E. C. Dickey, and C. A. Grimes, *Adv. Mater.* **15**, 624 (2003).
- [11] M. A. Fox and M. T. Dulay, *Chem. Rev.* **93**, 341 (1993).
- [12] M. R. Hoffmann, S. T. Martin, W. Choi, and D. W. Bahnemann, *Chem. Rev.* **95**, 69 (1995).
- [13] A. Mills, G. Hill, S. Bhopal, I. P. Parkin, and S. A. O'Neill, *J. Photochem. Photobiol. A, Chem.* **160**, 185 (2003).
- [14] G. K. Mor, K. Shankar, O. K. Varghese, and C. A. Grimes, *J. Mater. Res.* **19**, 2989 (2004).
- [15] B. M. Reddy et al., *J. Mol. Cat. A, Chem.* **223**, 295 (2004).
- [16] H. D. Jangl et al., *J. Nanoparticle Res.* **3**, 141 (2001).
- [17] T. Minabe, D. A. Tryk, P. Sawunyama, Y. Kikuchi, K. Hashimoto, and A. Fujishima, *J. Photochem. Photobiol. A, Chem.* **137**, 53 (2000).
- [18] G. K. Mor, K. Shankar, M. Paulose, O. K. Varghese, and C. A. Grimes, *Nano Lett.* **5**, 191 (2005).
- [19] M. Grätzel, *J. Photochem. Photobiol. C, Photochem. Rev.* **4**, 145 (2003).
- [20] J. H. Park, S. Kim, and A. J. Bard, *Nano Lett.* **6**, 24 (2006).
- [21] M. Grätzel, *Nature* **414**, 338–344 (2001).
- [22] C. Longo and M. A. De Paoli, *J. Braz. Chem. Soc.* **14**, 889 (2003).
- [23] J. M. Macák, H. Tsuchiya, A. Ghicov, and P. Schmuki, *Electrochem. Commun.* **7**, 1133 (2005).
- [24] G. K. Mor, K. Shankar, M. Paulose, O. K. Varghese, and C. A. Grimes, *Nano Lett.* **6**, 215 (2006).
- [25] G. K. Mor, O. K. Varghese, M. Paulose, K. Shankar, and C. A. Grimes, *Sol. Energy Mater. Sol. Cells* **90**, 2011 (2006).
- [26] X. Wang, M. Fujimaki, and K. Awazu, *Opt. Express* **13**, 1486 (2005).
- [27] J. Zhao, X. Wang, R. Chen, and L. Li, *Solid State Commun.* **134**, 705 (2005).
- [28] G. K. Mor, O. K. Varghese, M. Paulose, N. Mukherjee, and C. A. Grimes, *J. Mater. Res.* **18**, 2588 (2003).
- [29] J. Choi, R. B. Wehrspohn, J. Lee, and U. Gösele, *Electrochim. Acta* **49**, 2645 (2004).
- [30] J. M. Macak, H. Tsuchiya, and P. Schmuki, *Angew. Chem., Int. Ed.* **44**, 2100 (2005).
- [31] J. M. Macak, H. Tsuchiya, L. Taveira, S. Aldabergerova, P. Schmuki et al., *Angew. Chem., Int. Ed.* **44**, 7463 (2005).
- [32] L. V. Taveira, J. M. Macák, H. Tsuchiya, L. F. P. Dick, and P. Schmuki, *J. Electrochem. Soc.* **152**, B405 (2005).
- [33] J. M. Macak, K. Sirotna, and P. Schmuki, *Electrochim. Acta* **50**, 3679 (2005).
- [34] Q. Cai, M. Paulose, O. K. Varghese, and C. A. Grimes, *J. Mater. Res.* **20**, 230 (2005).
- [35] O. K. Varghese, D. Gong, M. Paulose, C. A. Grimes, and E. C. Dickey, *J. Mater. Res.* **18**, 156 (2003).
- [36] H. Tsuchiya, J. M. Macák, A. Ghicov, L. Taveira, and P. Schmuki, *Corros. Sci.* **47**, 3324 (2005).
- [37] N.-G. Park, J. Van de Lagemaat, and A. J. Frank, *J. Phys. Chem. B* **104**, 8989 (2000).